First-order phase transition induced by quantum fluctuations in Heisenberg helimagnets

E. Rastelli
Dipartimento di Fisica dell'Università, 43100 Parma, Italy

A. B. Harris*
School of Physics and Astronomy, Tel Aviv University, Ramat Aviv, 69978, Tel Aviv, Israel
(Received 6 July 1988; revised manuscript received 8 December 1988)

We calculate the ground-state energy of an isotropic quantum Heisenberg ferromagnet on an hexagonal lattice with ferromagnetic exchange interactions J_1 and J' between nearest neighbors in the same basal plane and adjacent basal planes and, respectively, competing interactions J_2 and J_3 between second- and third-nearest neighbors in the same basal plane, respectively. When the ground-state energy of a helical state with wave vector $\mathbf{Q}$ is expanded for small Q as $E_G(\mathbf{Q})=E_0+E_2Q^2+E_4Q^4+\cdots$, then the coefficients E_2 and E_4 can be evaluated *exactly* at zero temperature, with the result that E_2 is given by its classical ($S\to\infty$) value, whereas E_4 has quantum corrections. At the ferromagnet-helix transition (at which $E_2=0$) E_4 is positive for $S=\infty$ indicating that this transition is continuous, whereas as S^{-1} is nonzero, a region develops wherein the transition becomes discontinuous.

I. INTRODUCTION

Helimagnetism is a widely studied subject both experimentally and theoretically.[1] Very rich phase diagrams can arise from competition between the exchange coupling of a spin to a different shell of its neighbors.[2] In particular, we consider a Heisenberg system of quantum spins of magnitude S on a simple hexagonal lattice governed by the Hamiltonian

$$H=-2\sum_{\langle i,j\rangle} J_{ij}\,\mathbf{S}_i\mathbf{S}_j\ , \tag{1}$$

where $\langle\cdots\rangle$ indicates that the sum is over pairs of neighbors i,j and the exchange interactions J_{ij} between spins on sites i and j are as follows. In a given basal plane first-nearest neighbors (FNN's) have a ferromagnetic interaction $J_1>0$, second-nearest neighbors (SNN's), and third-nearest neighbors (TNN's) have respective interactions J_2 and J_3 of either sign. Nearest neighbors (NN's) in adjacent basal planes whose separation vector lies along the crystal c axis (recall we treat a *simple* hexagonal lattice), are subject to a ferromagnetic interaction J'. In actual systems[3-5] J' is usually negative. However, for such actual systems the staggered magnetization for a model with $J'<0$ behaves similarly to the uniform magnetization for the simpler model considered here with $J'>0$. In the classical approximation, i.e., for $S\to\infty$, the phase diagram and the spin-wave excitation spectrum are well known.[2] The phase diagram at zero temperature in the parameter space $j_2=J_2/J_1$, $j_3=J_3/J_1$, shown in Fig. 1, is divided into five regions each with a different arrangement of spins in a given basal plane. (We will often use lower-case variables to represent the dimensionless or "reduced" version of the corresponding upper-case variables.) Within our model all spins along a line parallel to the crystal c axis are parallel to one another, since interplane coupling is ferromagnetic and only along this axis. The different types of ordering indicated in Fig. 1 are ferromagnetic (F), antiferromagnetic (AF) with antiparallel rows of FNN spins, helical (H) with either rows of parallel FNN spins (H_1) or rows of parallel SNN spins (H_2), and a three sublattice configuration (120°) in which there are three sublattices with spin directions separated by 120°. In the classical approximation the phase transitions are discontinuous except for the F-H transitions which are the object of the present investigation and the AF-H transition which will be discussed elsewhere. The phase boundaries are given by

$$j_2=-1,\quad F\text{-}AF\ , \tag{2a}$$

$$j_2=-(1+4j_3)/3,\quad F\text{-}H_1 \text{ or } F\text{-}H_2\ , \tag{2b}$$

$$j_3=-1,\quad F\text{-}120^\circ\ , \tag{2c}$$

$$j_2=1-4j_3,\quad AF\text{-}H_1\ , \tag{2d}$$

$$j_2=2j_3,\quad H_1\text{-}H_2\ , \tag{2e}$$

$$j_3=j_2^2/(1-2j_2),\quad H_2\text{-}120^\circ\ . \tag{2f}$$

The multicritical points (A and C in Fig. 1) where, respectively, the $F-AF-H$ and $F-H-120^\circ$ phases coexist are given by

$$j_2=-1,\quad j_3=\tfrac{1}{2},\quad F\text{-}AF\text{-}H\ , \tag{2g}$$

$$j_2=1,\quad j_3=-1,\quad F\text{-}H\text{-}120^\circ\ . \tag{2h}$$

These phases may be characterized by a wave vector $\mathbf{Q}$, such that $\mathbf{Q}\cdot(\mathbf{r}_i-\mathbf{r}_j)$ is the angle between the expectation value of the spin vectors at $\mathbf{r}_i$ and $\mathbf{r}_j$:

$$\mathbf{Q}(F)=(0,0,0)\ , \tag{3a}$$

$$\mathbf{Q}(AF)=(2\pi/(a\sqrt{3}),0,0)\ , \tag{3b}$$

$$\mathbf{Q}(H_1)=(2\cos^{-1}[-(1+j_2)/(2j_2+4j_3)]/(a\sqrt{3}),0,0)\ , \tag{3c}$$

$$\mathbf{Q}(H_2)=\left[0,2\cos^{-1}\left[\frac{2j_3-3j_2-[(2j_3+3j_2)^2-8j_3]^{1/2}}{8j_3}\right]\Big/a,0\right]\ , \tag{3d}$$

$$\mathbf{Q}(120°)=(0,4\pi/(3a),0)\ , \tag{3e}$$

where a is the nearest-neighbor separation in the basal plane and the x axis is taken to lie along an SNN direction, as shown in Fig. 2. The nature of the phase boundary separating the two helical phases has been studied,[6] but we shall postpone our discussion of it to a later paper.

The situation when quantum corrections are taken into account is more subtle. A previous analysis[7] of such corrections to the classical ground-state energy to first order in $1/S$ found substantial effects, namely a significant increase in the domain of existence of the AF phase at the expense of the F and H phases, but no change in the location of the F-H boundary. This treatment was subject to some uncertainty, however. First, it was not clear what the effect of terms of higher order in $1/S$ might be, and second, since the AF is actually stable in regimes where harmonic spin waves in the AF are unstable, a convenient starting point for perturbation theory in powers of $1/S$ does not exist. Recently[8] we presented a method of analysis in which these difficulties could in part, at least, be overcome. There, for a hexagonal lattice and $S=\infty$, one can write the ground-state energy E_G as a function of $\mathbf{Q}$ for small Q as[9]

$$E_G(\mathbf{Q})=E_0+E_2Q^2+E_4Q^4+\cdots+E_{6,6}Q^6\cos(6\theta_Q)\ , \tag{4}$$

where θ_Q is the angle between $\mathbf{Q}$ and $\hat{x}$, where we introduce an orthogonal set of unit vectors, $(\hat{x},\hat{y},\hat{z})$, fixed with respect to the crystal such that $\hat{z}$ lies along the crystal c axis, and $\hat{x}$, lies along a SNN direction. Note that due to the hexagonal symmetry, the anisotropy first enters at order Q^6. The sign of the sixth-order anisotropy determines which of the two helical phases occur; for $E_{6,6}>0$, $\mathbf{Q}\perp\hat{x}$ so that phase H_2 occurs, whereas for $E_{6,6}<0$, $\mathbf{Q}\parallel\hat{x}$, so that phase H_1 is stable. At the multicritical point B in Fig. 1, $E_{6,6}$ vanishes.

For a classical spin system, where exact calculations of $E_G(\mathbf{Q})$ can be performed, it is convenient, but not absolutely essential, to use the expansion of Eq. (4). The advantage of this formulation is that one readily identifies the parameters E_2, E_4, and $E_{6,6}$ which determine in large part the nature of the phase diagram. Thus the study of the phase diagram is reduced to an analysis of how these parameters depend on the J_{ij}. In contrast, for quantum systems an expansion in powers of Q^2 appears to be an essential simplification, for instance, when one calculates how $\mathbf{Q}_G$, the ground-state value of $\mathbf{Q}$, depends on the exchange parameters in the H phase near the F-H phase boundary where $E_2\to 0$. From Eq. (4) one sees that in that case, assuming E_4 to be positive, one has $Q_G^2\approx -E_2/(2E_4)$. This result incorporates correctly all quantum corrections in the limit $E_2\to 0$. Although we will not pursue this point further here, it is clear that a

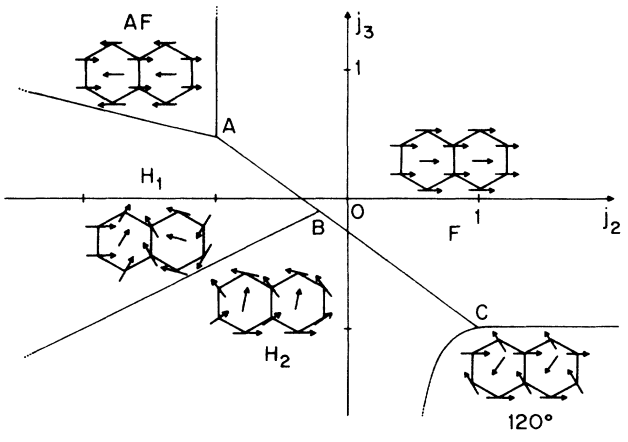

FIG. 1. Classical phase diagram of the Heisenberg system of Eq. (1) on a simple hexagonal lattice at zero temperature. The various phases are described in the text. Quantum corrections cause the F-H transition to become discontinuous for regions near the multicritical points A and C.

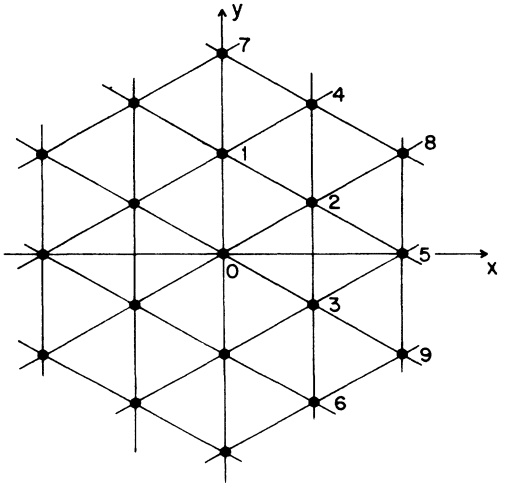

FIG. 2. Labeling of neighbors of a central spin (labeled 0) in a given basal plane. Neighbor no. 10 (not shown) lies in an adjacent basal plane at $\mathbf{r}=(0,0,c)$.

direct calculation of $\mathbf{Q}_G$ is more intricate than one based on Eq. (4).

We will return in future papers to discuss the H_1-H_2 and H_1-AF transitions. Here we consider the effects of quantum fluctuations on the F-H transition line. To this end we note that the expansion in Eq. (4) determines the nature of the phase transition. As a preliminary, we note that at temperature $T=0$, the spin magnitude in a helical state at zero temperature is close if not equal to S. Consequently, for the F-H transition to be continuous, it must be that $\mathbf{Q}$ in the H phase tends to zero as the phase boundary is approached. If $\mathbf{Q}$ is discontinuous, the transition is discontinuous. Now we apply a Landau-type argument to Eq. (4). If the transition is continuous, then E_4 in Eq. (4) must be positive at the phase boundary. In this case, the location of the phase boundary ABC in Fig. 1 is determined by the condition $E_2=0$. If, on the other hand, E_4 is negative when $E_2\rightarrow 0$, then the transition is surely discontinuous. Thus, a definitive discussion of the F-H phase boundary requires at least a calculation of the dependence of E_2 and E_4 on the exchange parameters J_{ij}. [It is possible that E_4 could be positive, but that higher-order terms in the expansion of Eq. (4) could still drive the transition discontinuous. We do not consider this possibility.] Previously,[8] we reported in brief form a calculation of this type for a set of parameters ($j_2=0$, $j_3=-\frac{1}{4}$) suitable to describe approximately $NiBr_2$, where a first-order transition occurs[3] at $T=22.8$ K between a low-temperature H_2 phase and an in-plane (F) phase at higher temperature. For that case we found that for the isotropic Heisenberg model the transition at zero temperature was continuous. However, in most helical systems the plane in which the spins lie is determined by some easy-plane anisotropy. At least for the classical model, the inclusion of such easy-plane anisotropy does not affect the analysis. Of course, within the easy plane there must be residual anisotropy which leads to a small number of crystallographically equivalent orientations which minimize this anisotropy energy, E_A. Previously,[8] we found that inclusion of E_A causes the transition to become discontinuous leading to a jump in $|\mathbf{Q}|$ proportional to E_A as the F-H phase boundary is crossed.

In the present paper we extend the analysis to treat the entire F-H phase boundary ABC of Fig. 1 and give a detailed description of the method. An important new conclusion of the present work is that E_4 becomes negative, i.e., the F-H transition is discontinuous, for a range of parameters near the multicritical point labeled A in Fig. 1. The size of the first-order region becomes smaller as either J' or S is increased, but even for $J'=J$ and $S=\frac{5}{2}$ the first-order region is quite significant, occurring for $j_3>0.36$. This work points out a possible advantage in studying quantum corrections in a controlled situation. Here these effects are governed by the expansion parameter, Q, which is arbitrarily small at the transition.

Briefly, this paper is organized as follows. In Sec. II we give details of the ladder approximation whereby the coefficient E_4 is evaluated exactly at $T=0$. The coefficient E_2 is shown to be given by its classical ($S=\infty$) value. In Sec. III the details of the evaluation for the hexagonal lattice we study are given. The range over which the transition is a first-order one is given as a function of the exchange constants. Finally, our conclusions and a discussion of possible experiments on relevant compounds are given in Sec. IV. A brief report of these results has been given previously.[10]

II. EXACT GROUND-STATE ENERGY OF A HELICAL HEISENBERG SPIN SYSTEM IN THE SMALL Q LIMIT

We treat the model of Eq. (1) assuming the ground state to be a helical state of wave vector $\mathbf{Q}$. Since this model is isotropic, the orientations of the spins are not subject to an overall constraint. Therefore we arbitrarily take the spins to lie in the basal plane. Also, since J' couples a spin ferromagnetically to a unique neighbor in an adjacent basal plane, $\mathbf{Q}$, which modulates the spin direction, must also lie in a basal plane. Of course, in the F state, $E_G(\mathbf{Q})$ will be greater than $E_G(0)$. However, this calculation will tell us whether or not the phase transition is continuous. Accordingly, we use the Dyson-Maleev[11,12] transformation to boson operators when spin components are taken with respect to local axes (ξ, η, ζ), defined so that the expectation value of $\mathbf{S}_i$ in the boson vacuum state lies along the local ζ_i axis. Thus,

$$S_i^x=-\sin(\mathbf{Q}\cdot\mathbf{r}_i)S_i^\eta+\cos(\mathbf{Q}\cdot\mathbf{r}_i)S_i^\xi\ , \tag{5a}$$

$$S_i^y=\cos(\mathbf{Q}\cdot\mathbf{r}_i)S_i^\eta+\sin(\mathbf{Q}\cdot\mathbf{r}_i)S_i^\xi\ , \tag{5b}$$

$$S_i^z=-S_i^\xi\ . \tag{5c}$$

The transformation to bosons[11,12] is then

$$S_i^+\equiv S_i^\xi+iS_i^\eta=\sqrt{2S}\,[1-a_i^\dagger a_i/(2S)]a_i\ , \tag{6a}$$

$$S_i^-\equiv S_i^\xi-iS_i^\eta=\sqrt{2S}\,a_i^\dagger\ , \tag{6b}$$

$$S_i^\zeta=S-a_i^\dagger a_i\ , \tag{6c}$$

where $[a_i,a_j^\dagger]=\delta_{i,j}$, in terms of the Kronecker delta. We introduce the spatial Fourier transforms by

$$a_{\mathbf{k}}^\dagger=N^{-1/2}\sum_i \exp(i\mathbf{k}\cdot\mathbf{r}_i)a_i^\dagger\ , \tag{7}$$

and the conjugate expression for $a_{\mathbf{k}}$, where N is the total number of spins. Using these relations the Hamiltonian of Eq. (1) then becomes

$$H=E_0(\mathbf{Q})+\sum_{\mathbf{k}} A_{\mathbf{k}}a_{\mathbf{k}}^{\dagger}a_{\mathbf{k}}+\tfrac{1}{2}\sum_{\mathbf{k}} B_{\mathbf{k}}(a_{\mathbf{k}}a_{-\mathbf{k}}+a_{\mathbf{k}}^{\dagger}a_{-\mathbf{k}}^{\dagger})-\frac{1}{\sqrt{2NS}}\sum_{1,2,3}\tfrac{1}{2}(C_2+C_3)\delta(1-2-3)(a_1^{\dagger}a_2a_3+a_2^{\dagger}a_3^{\dagger}a_1)$$
$$+\frac{1}{2NS}\sum_{1,2,3,4} V_{1234}\delta(1+2-3-4)a_1^{\dagger}a_2^{\dagger}a_3a_4-\frac{1}{2NS}\sum_{1,2,3,4}\tfrac{1}{3}(B_2+B_3+B_4)\delta(1-2-3-4)a_1^{\dagger}a_2a_3a_4$$
$$+\left[\frac{1}{2NS}\right]^{3/2}\sum_{1,2,3,4,5} C_{1-3}\delta(1+2-3-4-5)a_1^{\dagger}a_2^{\dagger}a_3a_4a_5$$
$$+\left[\frac{1}{2NS}\right]^{2}\sum_{1,2,3,4,5,6}\tfrac{1}{2}B_{1-5-6}\delta(1+2-3-4-5-6)a_1^{\dagger}a_2^{\dagger}a_3a_4a_5a_6\ , \tag{8}$$

where $a_1^{\dagger}=a_{\mathbf{k}_1}^{\dagger}$, $a_1=a_{\mathbf{k}_1}$, etc., and $E_0(\mathbf{Q})$ is the classical value of the energy of the spin state with modulation vector $\mathbf{Q}$ and is given by

$$E_0(\mathbf{Q})=-\sum_{\alpha} J_{\alpha}NS^2\sum_{\delta_\alpha}\cos\mathbf{Q}\cdot\boldsymbol{\delta}_{\alpha}-2J'NS^2\ . \tag{9}$$

Also

$$A_{\mathbf{k}}=\sum_{\alpha}2J_{\alpha}S\sum_{\delta_\alpha}[\cos\mathbf{Q}\cdot\boldsymbol{\delta}_{\alpha}-\tfrac{1}{2}\cos\mathbf{k}\cdot\boldsymbol{\delta}_{\alpha}(1+\cos\mathbf{Q}\cdot\boldsymbol{\delta}_{\alpha})]$$
$$+2J'S\sum_{\delta'}(1-\cos\mathbf{k}\cdot\boldsymbol{\delta}')\ , \tag{10}$$

$$B_{\mathbf{k}}=-\sum_{\alpha}J_{\alpha}S\sum_{\delta_\alpha}\cos\mathbf{k}\cdot\boldsymbol{\delta}_{\alpha}(1-\cos\mathbf{Q}\cdot\boldsymbol{\delta}_{\alpha})\ , \tag{11}$$

$$C_{\mathbf{k}}=\sum_{\alpha}2J_{\alpha}S\sum_{\delta_\alpha}\sin\mathbf{Q}\cdot\boldsymbol{\delta}_{\alpha}\sin\mathbf{k}\cdot\boldsymbol{\delta}_{\alpha}\ , \tag{12}$$

$$V_{1234}=-\tfrac{1}{4}[2(A_1+A_2)-D_{1-3}-D_{1-4}-D_{2-3}-D_{2-4}]\ , \tag{13}$$

where $\boldsymbol{\delta}_{\alpha}$ is a nearest-neighbor vector in the α shell of neighbors with corresponding exchange integral J_{α} and $D_{\mathbf{k}}=A_{\mathbf{k}}-B_{\mathbf{k}}$. We take the unperturbed Hamiltonian to be

$$H_0=E_0(\mathbf{Q})+\sum_{\mathbf{k}} A_{\mathbf{k}}a_{\mathbf{k}}^{\dagger}a_{\mathbf{k}}\ . \tag{14}$$

Then the ground-state energy is given by the perturbation expansion[13]

$$E_G(\mathbf{Q})=E_0(\mathbf{Q})+\left\langle 0\left|H'\sum_{n=0}^{\infty}\{[E_0(\mathbf{Q})-H_0]^{-1}H'\}^n\right|0\right\rangle_c\ , \tag{15}$$

where $H'=H-H_0$ is the perturbation and the subscript c means that only connected diagrams are to be included in the sum.

The statement that Eq. (8) is a Hamiltonian from which we will obtain the ground state associated with a given value of $\mathbf{Q}$ may at first sight seem paradoxical. For a finite system the transformations in Eqs. (5) and (6) merely amount to a specific choice of a representation within which the calculations are carried out. The eigenvalue spectrum, and in particular the ground-state energy, will be independent of the choice of representation, i.e., of the choice of $\mathbf{Q}$. Thus for a finite system, what we call $E_G(\mathbf{Q})$ is in fact simply the ground-state energy and is independent of $\mathbf{Q}$.

What then is the meaning of our calculation? We are considering an infinite system. Whereas, for the finite system, the value of $\mathbf{Q}$ initially chosen does not matter, for the infinite system, one finds no change in $\mathbf{Q}$ to any order of perturbation theory. Thus we believe that diagonalizing the Hamiltonian of Eq. (8) amounts to minimizing

$$\langle\Psi|H|\Psi\rangle/\langle\Psi|\Psi\rangle \tag{16}$$

not over all Ψ's (that would give the exact ground state), but rather over all Ψ's in the subspace of wave functions associated with wave vector $\mathbf{Q}$. In this regard the parameter $\mathbf{Q}$ functions like the lattice constant in a phonon calculation for an infinite lattice. There one imposes a lattice constant and in the end minimizes the energy with respect to this parameter.

We now consider the contributions from Eq. (15) to the coefficients E_2 and E_4 of Eq. (4). For this purpose we utilize the expansions for small wave vector:

$$E_0(\mathbf{Q})=-\sum_{\alpha}J_{\alpha}NS^2\sum_{\delta_\alpha}[1-\tfrac{1}{2}(\mathbf{Q}\cdot\boldsymbol{\delta}_{\alpha})^2+\tfrac{1}{24}(\mathbf{Q}\cdot\boldsymbol{\delta}_{\alpha})^4+\cdots]-2J'NS^2\ , \tag{17}$$

$$A_{\mathbf{k}}=\sum_{\alpha}2J_{\alpha}S\sum_{\delta_\alpha}[1-\cos\mathbf{k}\cdot\boldsymbol{\delta}_{\alpha}-\tfrac{1}{2}(\mathbf{Q}\cdot\boldsymbol{\delta}_{\alpha})^2(1-\tfrac{1}{2}\cos\mathbf{k}\cdot\boldsymbol{\delta}_{\alpha})+\cdots]+2J'S\sum_{\delta'}(1-\cos\mathbf{k}\cdot\boldsymbol{\delta}')\ , \tag{18}$$

$$B_{\mathbf{k}}=-\sum_{\alpha}J_{\alpha}S\sum_{\delta_\alpha}\tfrac{1}{2}(\mathbf{Q}\cdot\boldsymbol{\delta}_{\alpha})^2\cos\mathbf{k}\cdot\boldsymbol{\delta}_{\alpha}+\cdots\ , \tag{19}$$

$$C_{\mathbf{k}}=\sum_{\alpha}2J_{\alpha}S\sum_{\delta_\alpha}(\mathbf{Q}\cdot\boldsymbol{\delta}_{\alpha})\sin\mathbf{k}\cdot\boldsymbol{\delta}_{\alpha}+\cdots\ , \tag{20}$$

$$D_{\mathbf{k}}=\sum_{\alpha}2J_{\alpha}S\sum_{\delta_\alpha}(1-\cos\mathbf{k}\cdot\boldsymbol{\delta}_{\alpha})[1-\tfrac{1}{2}(\mathbf{Q}\cdot\boldsymbol{\delta}_{\alpha})^2+\ldots]+2J'S\sum_{\delta'}(1-\cos\mathbf{k}\cdot\boldsymbol{\delta}')\ . \tag{21}$$

First we note that the unperturbed ground state is the vacuum state containing no particles. Thus, of all the perturbation terms in Eq. (15) only those involving $a_{\mathbf{k}}^{\dagger}a_{-\mathbf{k}}^{\dagger}$ give a nonzero result when acting on the ground state. Similarly, the only terms in the perturbation which lead to a nonzero result for $\langle 0|H'$ are those involving $a_{\mathbf{k}}a_{-\mathbf{k}}$. Each of these terms carries with it a factor of $B_{\mathbf{k}}$, which by Eq. (19) is of order Q^2. Thus we conclude that there are *no* quantum corrections of order Q^2, i.e., E_2 is given correctly by its classical value. To order Q^4, i.e., to calculate E_4 completely, we may work to order $B_{\mathbf{k}}^2$ and set $\mathbf{Q}=0$ in all the other perturbations. For $\mathbf{Q}=0$ the perturbation reduces to that treated by Dyson[11] and Maleev[12] (DM) for the ferromagnet, i.e.,

$$H'(\mathbf{Q}=0)=(2NS)^{-1}\sum_{1,2,3,4}V_{1234}^{\mathrm{DM}}\delta(1+2-3-4)\times a_1^{\dagger}a_2^{\dagger}a_3a_4\ , \tag{22a}$$

where

$$V_{1234}^{\mathrm{DM}}=\tfrac{1}{4}(A_{1-3}+A_{1-4}+A_{2-3}+A_{2-4}-2A_1-2A_2)\ , \tag{22b}$$

where from now on we set $\mathbf{Q}=0$ in Eq. (18) for $A_{\mathbf{k}}$. Accordingly, to calculate E_4 we only need to consider the perturbation of Eq. (22a), which is represented in Fig. 3(a) by a four-point vertex with two incoming and two outgoing lines, and the perturbation involving $B_{\mathbf{k}}$, which is represented in Fig. 3(a) by vertices with either two incoming lines or two outgoing lines. Thus the *complete* perturbation series for E_4 reduces to that shown diagrammatically in Fig. 3(c). Because of momentum conservation, each rung of the ladder must consist of two legs having equal and opposite momentum. Thus we have

$$\langle 0|H'[E_0(\mathbf{Q})-H_0]^{-1}H'|0\rangle_c=-\tfrac{1}{4}\sum_{\mathbf{k}_1}B_{\mathbf{k}_1}^2/A_{\mathbf{k}_1}\ , \tag{23a}$$

$$\langle 0|H'\{[E_0(\mathbf{Q})-H_0]^{-1}H'\}^2|0\rangle_c=(8NS)^{-1}\sum_{\mathbf{k}_1,\mathbf{k}_2}B_{\mathbf{k}_1}V_{\mathbf{k}_1,\mathbf{k}_2}B_{\mathbf{k}_2}/(A_{\mathbf{k}_1}A_{\mathbf{k}_2})\ , \tag{23b}$$

where $V_{\mathbf{k},\mathbf{k}'}=V_{\mathbf{k},-\mathbf{k},\mathbf{k}',-\mathbf{k}'}$. The series consisting of arbitrary order iteration of diagrams of the type in Fig. 3(c) leads to the result

$$E_G(\mathbf{Q})=E_0(\mathbf{Q})-\tfrac{1}{4}\sum_{\mathbf{k}}B_{\mathbf{k}}^2/A_{\mathbf{k}}+(8NS)^{-1}\sum_{\mathbf{k},\mathbf{q}}B_{\mathbf{k}}B_{\mathbf{q}}T_{\mathbf{k},\mathbf{q}}/(A_{\mathbf{k}}A_{\mathbf{q}})\ , \tag{24}$$

where

$$T_{\mathbf{k},\mathbf{q}}=V_{\mathbf{k},\mathbf{q}}-(2NS)^{-1}\sum_{\mathbf{k}'}V_{\mathbf{k},\mathbf{k}'}T_{\mathbf{k}',\mathbf{q}}/A_{\mathbf{k}'}\ , \tag{25}$$

is the zero-momentum t matrix,[11,14,15] shown schematically in Fig. 3(b). We should emphasize that Eqs. (24) and (25) hold for more general lattice structures. They give correctly all terms in the ground-state energy of order Q^4.

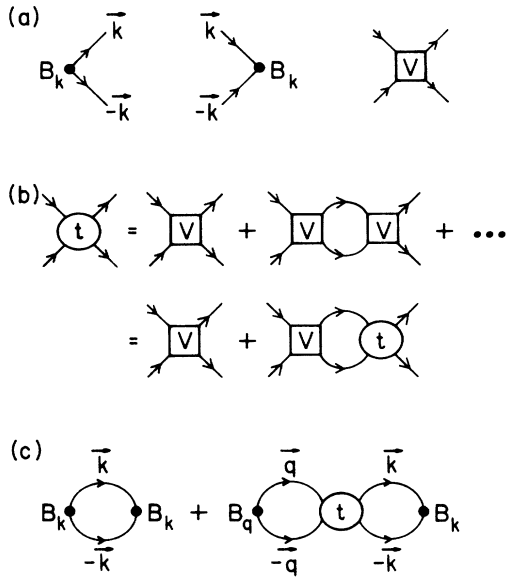

FIG. 3. Diagrammatic evaluation of the perturbation series. Shown are the diagrammatic representations of (a) the quadratic perturbations proportional to $B_{\mathbf{k}}$ and the quartic interaction $H'(Q=0)$ of Eq. (22a), (b) Eq. (25), and (c) Eq. (24).

III. APPLICATION TO THE HEXAGONAL HELIMAGNET

Let us consider a hexagonal Heisenberg helimagnet with the following in-plane interactions: FNN $J_1>0$, SNN J_2, TNN J_3, and an interaction $J'>0$ between out-of-plane NN's. Then the classical ground-state energy of Eq. (17) reduces to

$$\begin{aligned}E_0(\mathbf{Q})&=-6J_1NS^2[1+j_2+j_3+\tfrac{1}{3}j'\\&\quad-\tfrac{1}{4}(1+3j_2+4j_3)(aQ)^2\\&\quad+\tfrac{1}{64}(1+9j_2+16j_3)(aQ)^4]\\&\equiv 6J_1NS^2e_0(\mathbf{Q})\ ,\end{aligned} \tag{26}$$

where $j_2=J_2/J_1$, $j_3=J_3/J_1$, and $j'=J'/J_1$. Thus if one writes $E_2=6J_1NS^2e_2$ and $E_4=6J_1NS^2e_4$, then for $S=\infty$ one has

$$e_2(S=\infty)=\tfrac{1}{4}(1+3j_2+4j_3)a^2\ , \tag{27a}$$

$$e_4(S=\infty)=-\tfrac{1}{64}(1+9j_2+16j_3)a^4\ . \tag{27b}$$

We now implement the perturbative scheme outlined above to find the quantum corrections to e_4 for finite S. [As noted above, there are no such corrections to e_2, so Eq. (27a) gives $e_2(S)$ exactly for all S.] We set

$$A_{\mathbf{k}}=12J_1S\varepsilon_{\mathbf{k}}\ , \tag{28}$$

where

$$\varepsilon_{\mathbf{k}}=\tfrac{1}{3}\sum_{m=1}^{10}\hat{j}_m(1-\cos k_m),\quad m=1,2,\ldots,10\ , \tag{29}$$

with

$$\hat{j}_1=\hat{j}_2=\hat{j}_3=1 , \tag{30a}$$

$$\hat{j}_4=\hat{j}_5=\hat{j}_6=j_2 , \tag{30b}$$

$$\hat{j}_7=\hat{j}_8=\hat{j}_9=j_3 , \tag{30c}$$

$$\hat{j}_{10}=j' , \tag{30d}$$

and $k_m=\mathbf{k}\cdot\boldsymbol{\delta}_m$. The numbering of the neighbor vectors $\boldsymbol{\delta}_m$ for Eq. (29) and below is shown in Fig. 2. Also

$$B_{\mathbf{k}}=-12J_1S[\tfrac{1}{4}b_{\mathbf{k}}^{(1)}(aQ_x)^2+\tfrac{1}{4}b_{\mathbf{k}}^{(2)}(aQ_y)^2+\tfrac{1}{2}\eta_{\mathbf{k}}a^2Q_xQ_y] , \tag{31}$$

where

$$b_{\mathbf{k}}^{(1)}=\tfrac{1}{4}\cos k_2+\tfrac{1}{4}\cos k_3+j_2(\tfrac{1}{4}\cos k_4+\tfrac{1}{4}\cos k_6+\cos k_5)+j_3(\cos k_8+\cos k_9) , \tag{32a}$$

$$b_{\mathbf{k}}^{(2)}=\tfrac{1}{3}\cos k_1+\tfrac{1}{12}\cos k_2+\tfrac{1}{12}\cos k_3+\tfrac{3}{4}j_2(\cos k_4+\cos k_6)+\tfrac{1}{3}j_3(4\cos k_7+\cos k_8+\cos k_9) , \tag{32b}$$

$$\eta_{\mathbf{k}}=(\sqrt{3}/12)[\cos k_2-\cos k_3+3j_2(\cos k_4-\cos k_6)+4j_3(\cos k_8-\cos k_9)] . \tag{32c}$$

Substituting Eqs. (28) and (31) into (23a) we find that

$$\langle 0|H'[E_0(\mathbf{Q})-H_0]^{-1}H'|0\rangle_c=-6J_1NS[I_0^x(aQ_x)^4+I_0^y(aQ_y)^4+2I_0^{xy}(a^2Q_xQ_y)^2]/32 , \tag{33}$$

where

$$I_0^x=\frac{1}{N}\sum_{\mathbf{k}}[b_{\mathbf{k}}^{(1)}]^2/\varepsilon_{\mathbf{k}} , \tag{34a}$$

$$I_0^y=\frac{1}{N}\sum_{\mathbf{k}}[b_{\mathbf{k}}^{(2)}]^2/\varepsilon_{\mathbf{k}} , \tag{34b}$$

$$I_0^{xy}=\frac{1}{N}\sum_{\mathbf{k}}[b_{\mathbf{k}}^{(1)}b_{\mathbf{k}}^{(2)}+2\eta_{\mathbf{k}}^2]/\varepsilon_{\mathbf{k}} . \tag{34c}$$

For the symmetry of the hexagonal lattice, it is clear from Eq. (33) that we must have $I_0^x=I_0^y=I_0^{xy}\equiv I_0$, so that

$$\langle 0|H'[E_0(\mathbf{Q})-H_0]^{-1}H'|0\rangle_c=-6J_1NSI_0(aQ)^4/32 . \tag{35}$$

Now we turn to the evaluation of the contributions involving the t matrix, which we only need for zero total momentum and for $\mathbf{Q}=0$. Thus we write

$$V_{\mathbf{q},\mathbf{k}}=12J_1Sv_{\mathbf{q},\mathbf{k}} , \tag{36}$$

where

$$v_{\mathbf{q},\mathbf{k}}=\tfrac{1}{2}(\varepsilon_{\mathbf{q}-\mathbf{k}}+\varepsilon_{\mathbf{q}+\mathbf{k}})-\varepsilon_{\mathbf{q}} . \tag{37}$$

To take full advantage of the symmetry of the interaction, we introduce the following quantity

$$\tilde{v}_{\mathbf{q},\mathbf{k}}=\tfrac{1}{2}(\varepsilon_{\mathbf{q}-\mathbf{k}}+\varepsilon_{\mathbf{q}+\mathbf{k}})-\varepsilon_{\mathbf{q}}-\varepsilon_{\mathbf{k}} =-\tfrac{1}{3}\sum_{m=1}^{10}\hat{j}_m(1-\cos q_m)(1-\cos k_m) \tag{38a}$$

$$=v_{\mathbf{q},\mathbf{k}}-\varepsilon_{\mathbf{k}} . \tag{38b}$$

Because of the relations $\sum_{\mathbf{k}}B_{\mathbf{k}}=0$ and $N^{-1}\sum_{\mathbf{q}}v_{\mathbf{q},\mathbf{k}}=-\varepsilon_{\mathbf{k}}$, we may replace v by $\tilde{v}$ in the perturbation series of Eq. (24). Thus we rewrite Eqs. (24) and (25) as

$$E_G(\mathbf{Q})=E_0(\mathbf{Q})-\tfrac{3}{16}J_1NSI_0(aQ)^4+(8NS)^{-1}\sum_{\mathbf{q},\mathbf{k}}B_{\mathbf{k}}B_{\mathbf{q}}\tilde{t}_{\mathbf{q},\mathbf{k}}/(12J_1S\varepsilon_{\mathbf{k}}\varepsilon_{\mathbf{q}}) , \tag{39}$$

where we have used Eq. (35) and

$$\tilde{t}_{\mathbf{q},\mathbf{k}}=\tilde{v}_{\mathbf{q},\mathbf{k}}-(2NS)^{-1}\sum_{\mathbf{k}'}\tilde{v}_{\mathbf{q},\mathbf{k}'}\tilde{t}_{\mathbf{k}',\mathbf{k}}/\varepsilon_{\mathbf{k}'} . \tag{40}$$

We may write the solution to Eq. (40) as

$$\tilde{t}_{\mathbf{q},\mathbf{k}}=-\tfrac{1}{3}\sum_{m,n=1}^{10}\hat{j}_m(1-\cos q_m)(A^{-1})_{mn}(1-\cos k_n) , \tag{41}$$

where the matrix $\underline{A}$ is

$$A_{mn}=\delta_{m,n}-\hat{j}_nD_{mn}/(2S) , \tag{42}$$

with

$$D_{mn}=(3N)^{-1}\sum_{\mathbf{k}}(1-\cos k_m)(1-\cos k_n)/\varepsilon_{\mathbf{k}} . \tag{43}$$

The D_{mn} are calculated explicitly in Appendix A. Substitution of Eq. (41) into Eq. (39) gives

$$E_G(\mathbf{Q})=E_0(\mathbf{Q})-\tfrac{3}{16}J_1NSI_0(aQ)^4+6J_1N[I_1^x(aQ_x)^4+I_1^y(aQ_y)^4+2I_1^{xy}a^4Q_x^2Q_y^2]/64 , \tag{44}$$

where

$$I_1^x=-\tfrac{1}{3}\sum_{m,n=1}^{10}\hat{j}_m(A^{-1})_{mn}I_m^{(1)}I_n^{(1)} , \tag{45a}$$

$$I_1^y=-\tfrac{1}{3}\sum_{m,n=1}^{10}\hat{j}_m(A^{-1})_{mn}I_m^{(2)}I_n^{(2)} , \tag{45b}$$

$$I_1^{xy}=-\tfrac{1}{3}\sum_{m,n=1}^{10}\hat{j}_m(A^{-1})_{mn}\times[\tfrac{1}{2}(I_m^{(1)}I_n^{(2)}+I_m^{(2)}I_n^{(1)})+2I_m^{\eta}I_n^{\eta}] , \tag{45c}$$

with

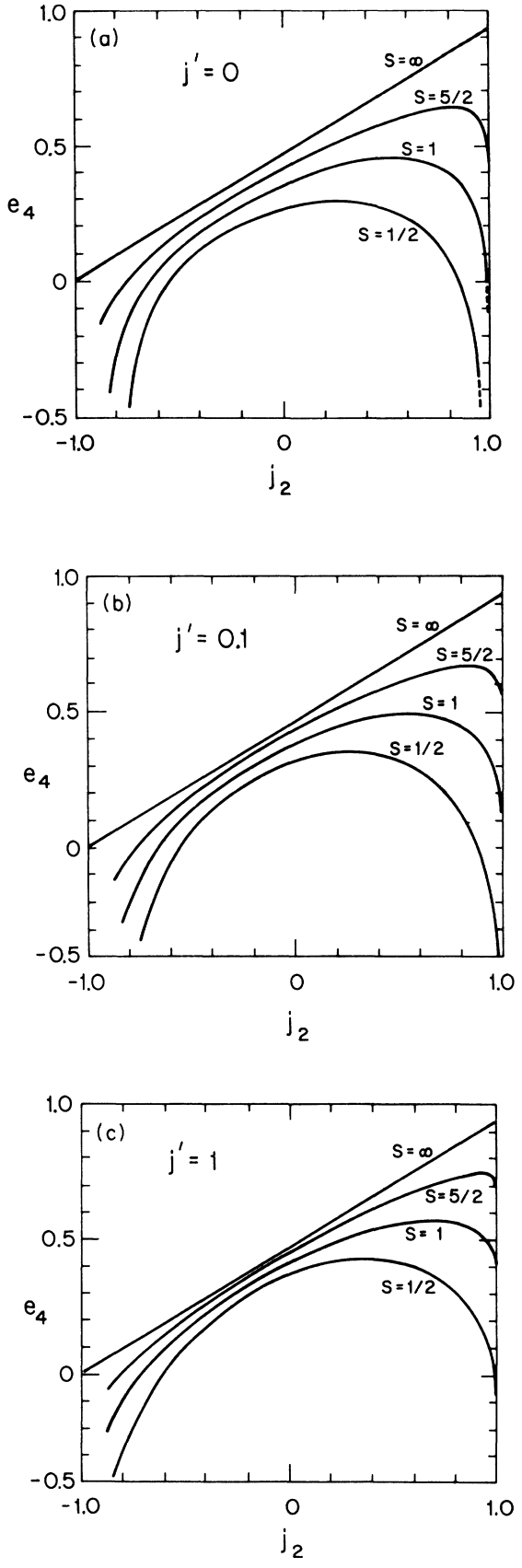

FIG. 4. e_4 as a function of j_2 along the F-H line (a) for $j'=0$, (b) for $j'=0.1$, and (c) for $j'=1$, for selected values of spin S.

$$I_m^{(i)}=\frac{1}{N}\sum_{\mathbf{k}} b_{\mathbf{k}}^{(i)}(1-\cos k_m)/\varepsilon_{\mathbf{k}},\quad i=1,2\ , \tag{46a}$$

$$I_m^{\eta}=\frac{1}{N}\sum_{\mathbf{k}} \eta_{\mathbf{k}}(1-\cos k_m)/\varepsilon_{\mathbf{k}}\ . \tag{46b}$$

The explicit calculation of $I_m^{(i)}$ and I_m^{η} is given in Appendix A. Consistent with the symmetry of the hexagonal lattice we have $I_1^x=I_1^y=I_1^{xy}\equiv I_1$, so that in all we have

$$E_G(\mathbf{Q})=E_0(\mathbf{Q})-6J_1NS[I_0-I_1/(2S)](aQ)^4/32 \tag{47}$$

correct to order Q^4. The reduced ground-state energy, $e(\mathbf{Q})\equiv E_G(\mathbf{Q})/(6J_1NS^2)$ along the F-H boundary line is

$$e(\mathbf{Q})=e_0+e_4(aQ)^4\ , \tag{48}$$

where

$$e_0=-\tfrac{3}{4}-\tfrac{1}{4}j_2-\tfrac{1}{3}j'\ , \tag{49a}$$

$$e_4=\tfrac{1}{32}\left[\tfrac{3}{2}+\tfrac{3}{2}j_2-\frac{I_0}{S}+\frac{I_1}{2S^2}\right]\ . \tag{49b}$$

In Fig. 4 we show the coefficient e_4 of the Q^4 contribution versus j_2 for $j'=0,0.1,1$, and for selected values of the spin S.

As one can see, for each finite value of S two intervals on the F-H phase boundary where E_4 is negative appear near the terminal points A ($j_2=-1$, $j_3=\frac{1}{2}$) and C ($j_2=1$,

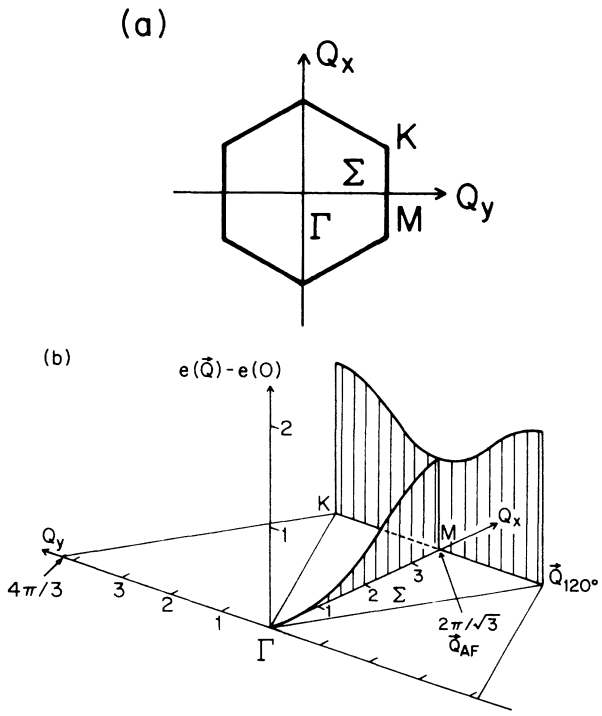

FIG. 5. (a) $Q_z=0$ plane of the Brillouin zone in the notation of Koster (Ref. 16). The Γ point corresponds to the F phase, M to the AF phase, and K to the 120° phase. (b) Spin-wave energy vs wave vector in the basal plane showing the minimum at $Q=0$, the saddle point at M and the maximum at K. These curves are for a system on the H-F phase boundary near the F-H-AF multicritical point. Exactly at that multicritical point the spin-wave energy vanishes along the entire Σ line.

$j_3=-1$). Thus, in these intervals, the line $E_2=0$ defines not the phase boundary, but the limit of local stability of the F phase with respect to long-wavelength modulations. The actual phase transition is expected to be discontinuous and to occur for larger values of j_2 than on the line ABC of Fig. 1. One can see that these first-order regions become larger as (1) S is decreased, i.e., as we get further from the classical limit, and (2) j' is decreased (so that spin-wave fluctuations are enhanced). Also, the quantum effect on E_4 is more dramatic near the point A where the AF, H, and F phases coexist than near the point C where the 120°, H, and F phases coexist. This result can be understood by consideration of the nature of the spin-wave spectra at points A and C. At point A the spin waves have zero energy for all[2] wave vectors along the line Σ in Fig. 5(a), corresponding to the instability associated with uniformly rotating a suitable line of spins. In Fig. 5(b) we show the spin-wave energy for wave vectors as indicated in Fig. 5(a) for a point on the F-H phase boundary near point A. As point A is approached the instability along the entire line Σ develops. Thus one has a "soft direction" which leads to a divergence in E_4 as the point A is approached. In contrast, the spin-wave spectrum at point C develops only a "pointwise" instability. At C the spin-wave energy vanishes at those wave vectors equivalent to the point K in Fig. 5(a), but there is no unstable line of spin waves as at point A.

The above discussion implicitly assumes that when quantum fluctuations are taken into account, the points (which we denote A' and C') where E_4 passes through zero actually remain in the regime of the F-H transition. This possibility is the first of the two scenarios shown in Fig. 6. This possibility will occur if the shift in the multicritical point (A or C) due to quantum fluctuations is smaller than the region (extending from A to A' or from C to C') over which E_4 is calculated to be negative. As we discuss in Appendix B, this is believed to be the case for the multicritical point A, so that the scenario in Fig. 6(a) is what we believe happens except for $S=\frac{1}{2}$ and for very small values of j'. Typical results for A' and A'' are shown in Fig. 7. On the other hand, for point C, where the interval C-C' is very small, this seems not to be the

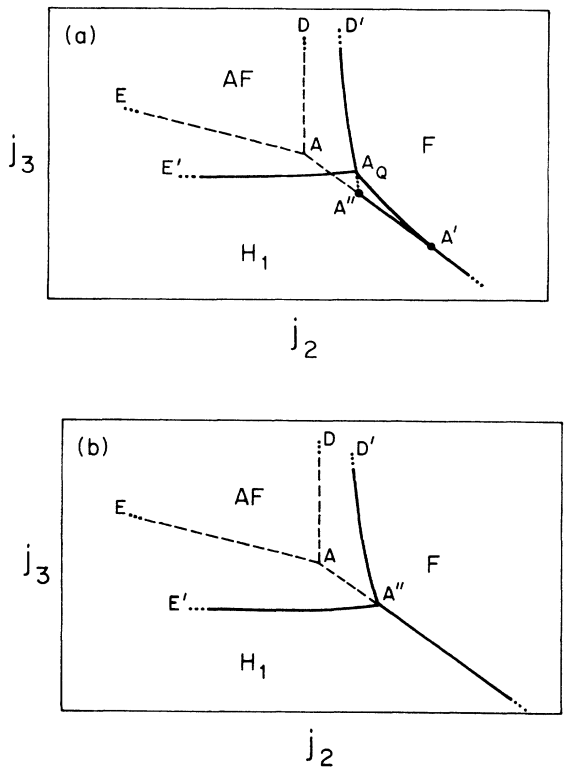

FIG. 6. Two scenarios (a) and (b) for the modification of the phase diagram for the classical model by the presence of quantum fluctuations. The classical phase boundaries (as in Fig. 1) are shown by dashed lines. The F-H phase transition is continuous except in the interval A'-A_Q where quantum fluctuations cause it to be discontinuous. The point A'' is defined as the the point where the extrapolated F-AF phase boundary intersects the classical F-H transition line. In scenario (a) A' lies outside the interval A-A''. In scenario (b) A' (not shown) lies in the interval A-A''.

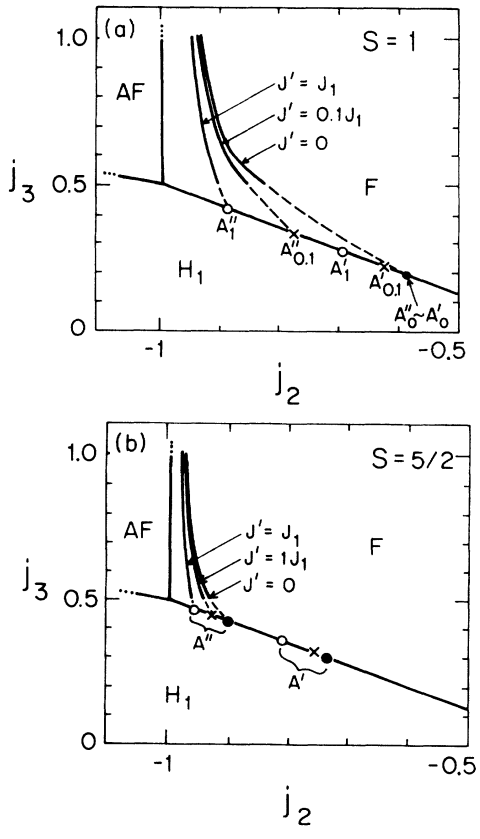

FIG. 7. Estimated locations of the points A' and A'' (see Fig. 6) to order $1/S$, as obtained in Appendix B, for various values of J' and for (a) $S=1$ and (b) $S=\frac{5}{2}$. Here the solid lines represent the AF-F phase boundary calculated to first order in $1/S$ according to Eq. (B9). For $j_3<0.5$ this calculation is not defined, and we use the extrapolation indicated by dashed lines. Also shown are the values of A' (to order $1/S$) on the F-H phase boundary where $e_4=0$. In (a) the subscripts on A' and A'' indicate the values of $j'\equiv J'/J_1$. In both panels the A' and A'' points are indicated by open circles for $j'=1$, crosses for $j'=0.1$ and solid circles for $j'=0$.

case. Thus we expect that the nature of the phase diagram near point C is not qualitatively modified by quantum fluctuations and one has a scenario analogous to that of Fig. 6(b). At present we are analyzing the H_1-H_2 and H_1-AF phase boundaries more carefully to see what the effects of quantum fluctuations for them are.

IV. EXPERIMENTAL POSSIBILITIES AND CONCLUSIONS

We now discuss possible systems on which experiments might establish the existence of the "quantum helix" we have found in this paper. The best candidates are transition metal halide insulators like $NiBr_2$, NiI_2, and CoI_2 which have helical spin ground states. In the nickel halides the effective spin is $S=1$, while in cobalt halides the effective spin is $S=\frac{1}{2}$ so that quantum effects could play an important role. To experimentally verify that quantum fluctuations have driven the H-F transition discontinuous one needs a system that (a) has an H-F transition at low temperature and (b) has exchange parameters near the point A in Fig. 1 so that quantum fluctuations are strong.

First consider $NiBr_2$. This compound is a widely studied one on which both elastic[3,4] and inelastic neutron scattering[17,18] have been performed. Also magnetization and susceptibility measurements of $NiBr_2$ under pressure have been performed.[19,20] At low temperature (0–23 K) $NiBr_2$ is a H_2-type helimagnet with a **Q** wave vector such that the turn angle between spins belonging to adjacent next-nearest-neighbor lines varies[3] from 9.7° at $T=0$ to 3° at $T_{H\to F}=23$ K where a "weak" first-order phase transition is observed to a collinear phase. Long-range order disappears at $T=44$ K. The transition temperature $T_{H\to F}$ is severely reduced under pressure[19,20] so that $NiBr_2$ under pressure can be made to satisfy condition (a), above. The values of the reduced exchange couplings in the low-temperature H_2 phase are inferred[17] to be $j_2=0$, $j_3=-0.28$. As one can see this point falls in the vicinity of the F-H line of Fig. 1 in the region where H_2 phase is stable and quantum effects do not change the order of the phase transition. The small discontinuity of the **Q** wave vector observed experimentally[3] at $T=23$ K can be explained[8] in terms of a very small lattice anisotropy, so that condition (b) is not satisfied. However, by suitable doping with Fe we may satisfy this condition. In $NiBr_2$ with Fe-neutron scattering[21] shows that although the helix wave vector for pure $NiBr_2$ corresponds to an H_2 phase for concentrations in the range 2–5.4 % the orientation of **Q** changes to that corresponding to the H_1 phase. Note that this concentration of Fe is low enough to treat the randomly diluted system as a pure one with effective exchange couplings. The obvious conclusion is that Fe doping drives the system towards the desired point A in Fig. 1, and thus by doping we may satisfy condition (b) above.

Next we consider NiI_2 and CoI_2. For these systems it may be easier to satisfy condition (b) but harder to satisfy condition (a). Elastic neutron scattering[5] on NiI_2 shows that it is a H_1-type helimagnet at low temperature and becomes a paramagnet at $T=75$ K. The turn angle between spins on adjacent NN lines is 49.8°. Since no inelastic neutron scattering measurements have been performed on this compound, all that one can do[5] is to locate NiI_2 along a straight line in Fig. 1 going from the triple point A to a point ($j_2=-0.28$, $j_3=-0.14$) on the H_1-H_2 transition line not far from point B. The same considerations hold[5] for CoI_2, a H_1 helimagnet with a turn angle of 45° that becomes a paramagnet at $T=8$ K. In any event, these systems are closer to point A than is $NiBr_2$. As in the case of $NiBr_2$ one might study Fe doping to see if such doped systems would be closer to point A, thus satisfying condition (b). As for condition (a), in neither NiI_2 nor CoI_2 has an H-F transition been seen. Thus the temperature, $T_{H\to F}$ at which the helix becomes unstable relative to the ferromagnetic phase must be higher than T_c, the temperature of the helix to paramagnet transition. However, if $NiBr_2$ is a guide, we expect that $T_{H\to F}$ will decrease strongly with applied pressure, so that under suitable pressure an H-F transition will occur and, hopefully, can be driven close to zero temperature to satisfy condition (a).

In attributing a first-order transition to quantum fluctuations one should note the following. The H-F transition should be continuous on the basis of the classical approximation, but it has to be first order on the basis of our results, if the exchange parameters j_2 and j_3 are not too far from point A of Fig. 1 [see point A' of Fig. 6(a) and Table I for $j'=0.1$]. Notice that in NiI_2 and CoI_2 the magnitude of the **Q** wave vector is much larger than that of $NiBr_2$ so that if this strong discontinuity should persist at the H-F transition, it could not be explained

TABLE I. Value of A' to all orders in $1/S$ for various values of $j'\equiv J'/J$ and spin S.

	$j'=0$		$j'=0.1$		$j'=1$	
	j_2	j_3	j_2	j_3	j_2	j_3
S						
$\frac{1}{2}$	a	a	−0.557	0.168	−0.613	0.210
1	−0.641	0.231	−0.659	0.244	−0.711	0.283
$\frac{3}{2}$	−0.695	0.271	−0.711	0.283	−0.762	0.321
2	−0.729	0.297	−0.744	0.308	−0.795	0.346
$\frac{5}{2}$	−0.755	0.316	−0.769	0.327	−0.817	0.363
∞	−1	$\frac{1}{2}$	−1	$\frac{1}{2}$	−1	$\frac{1}{2}$

[a]For this set of J_{ij}'s we do not give a value for A' since this point lies inside the interval A-A'' and hence does not correspond to a thermodynamical phase transition.

with a very small lattice anisotropy as in $NiBr_2$.

The following conclusions emerge from our results.

(1) We have given an *exact* calculation at zero temperature of the coefficients E_0, E_2, and E_4 in the expansion of the ground-state energy in powers of the helix wave vector $\mathbf{Q}$: $E_G(\mathbf{Q})=E_0+E_2Q^2+E_4Q^4+\cdots$. Near the ferromagnet-helix-antiferromagnet multicritical point we find that $E_4<0$ from which we conclude that the *F-H* phase transition becomes discontinuous near that multicritical point.

(2) The scheme we use is potentially of use in other contexts. First, one might make analogous, but perhaps less controlled, calculations for wave vectors close to that of the *AF* phase to determine whether quantum fluctuations can also cause that transition to become discontinuous. Secondly, the limit $Q\to 0$ provides a way of "turning on," i.e., gradually introducing quantum effects.

ACKNOWLEDGMENTS

We thank V. Fleurov for raising questions which the discussion of Eq. (16) is meant to answer. E.R. acknowledges partial support from the Ministry of Education (MPI) and from the Gruppo Nazionale di Struttura della Materia, CNR (GNSM). A.B.H. would like to acknowledge the School of Physics and Astronomy of Tel Aviv University for its hospitality. Partial support by grants from the US–Israel Binational Science Foundation, from the Israel Academy of Sciences and Humanities, from the Israel Atomic Energy Commission (IAEC), and from the National Science Foundation (NSF) under Grant No. 85-20272 are gratefully acknowledged.

APPENDIX A: NUMERICAL CALCULATIONS

In this appendix we show the explicit calculation of the integrals D_{mn}, I_0, and $I_m^{(1)}$, given, respectively, in Eqs. (43), (34), and (46a). Due to the symmetry of the threefold axis we have the relations

$$D_{1,1}=D_{2,2}=D_{3,3}\ , \tag{A1}$$

$$D_{1,2}=D_{1,3}=D_{2,3}\ , \tag{A2}$$

$$D_{1,4}=D_{1,6}=D_{2,4}=D_{2,5}=D_{3,5}=D_{3,6}\ , \tag{A3}$$

$$D_{1,5}=D_{2,6}=D_{3,4}\ , \tag{A4}$$

$$D_{1,7}=D_{2,8}=D_{3,9}\ , \tag{A5}$$

$$D_{1,8}=D_{1,9}=D_{2,7}=D_{2,9}=D_{3,7}=D_{3,8}\ , \tag{A6}$$

$$D_{4,4}=D_{5,5}=D_{6,6}\ , \tag{A7}$$

$$D_{4,5}=D_{4,6}=D_{5,6}\ , \tag{A8}$$

$$D_{4,7}=D_{4,8}=D_{5,8}=D_{5,9}=D_{6,7}=D_{6,9}\ , \tag{A9}$$

$$D_{4,9}=D_{5,7}=D_{6,8}\ , \tag{A10}$$

$$D_{7,7}=D_{8,8}=D_{9,9}\ , \tag{A11}$$

$$D_{7,8}=D_{7,9}=D_{8,9}\ , \tag{A12}$$

$$D_{1,10}=D_{2,10}=D_{3,10}\ , \tag{A13}$$

$$D_{4,10}=D_{5,10}=D_{6,10}\ , \tag{A14}$$

$$D_{7,10}=D_{8,10}=D_{9,10}\ . \tag{A15}$$

Thus only the D_{mn} appearing on the leftmost sides of the preceding equations are distinct. One notes also the sum rules

$$D_{1,1}+2D_{1,2}+j_2(2D_{1,4}+D_{1,5})+j_3(D_{1,7}+2D_{1,8})+j'D_{1,10}=1\ , \tag{A16a}$$

$$D_{1,5}+2D_{1,4}+j_2(2D_{4,5}+D_{5,5})+j_3(D_{5,7}+2D_{5,5})+j'D_{5,10}=1\ , \tag{A16b}$$

$$D_{1,7}+2D_{1,8}+j_2(D_{5,7}+2D_{5,8})+j_3(D_{7,7}+2D_{7,8})+j'D_{7,10}=1\ , \tag{A16c}$$

$$3D_{1,10}+3j_2D_{5,10}+3j_3D_{7,10}+j'D_{10,10}=1\ . \tag{A16d}$$

In order to perform numerical calculations we manipulate sums over the Brillouin zone into the form

$$\frac{1}{N}\sum_{\mathbf{k}} f(\mathbf{k})=(2\pi)^{-3}\int_{-\pi}^{\pi}\int_{-\pi}^{\pi}\int_{-\pi}^{\pi} dx\,dy\,dz\,f(x,y,z)\ , \tag{A17}$$

where $x=\sqrt{3}ak_x/2$, $y=ak_y/2$, and $z=ck_z$. In terms of these variables we have

$$\varepsilon_{\mathbf{k}}=\varepsilon(x,y)+j'(1-\cos z)/3\ , \tag{A18}$$

where

$$\varepsilon(x,y)=1-(\cos 2y+2\cos x\cos y)/3+j_2[1-(\cos 2x+2\cos x\cos 3y)/3]+j_3[1-(\cos 4y+2\cos 2x\cos 2y)/3]\ . \tag{A19}$$

The numerators of D_{mn} are independent of z, so that the integration over that variable can be done first:

$$(2\pi)^{-1}\int_{-\pi}^{\pi}\varepsilon_{\mathbf{k}}^{-1}\,dz=D(x,y)^{-1}\ , \tag{A20}$$

where

$$D(x,y)=\{\varepsilon(x,y)[\varepsilon(x,y)+2j'/3]\}^{1/2}\ . \tag{A21}$$

We use this relation to construct the D_{mn}. Furthermore, the $D_{m,10}$ can be determined in terms of the other D_{mn} via the sum rules of Eq. (A16).

By use of Eqs. (A20) we obtain

$$I_0=\frac{1}{4\pi^2}\int_0^{\pi}\int_0^{\pi} dx\,dy[b_1(x,y)]^2/D(x,y)\ , \tag{A22}$$

where

$$b_1(x,y)=\cos x\cos y+j_2(\cos x\cos 3y+2\cos 2x)+4j_3\cos 2x\cos 2y \tag{A23a}$$

and

$$I_1=-\tfrac{1}{3}\sum_{m,n=1}^{10} j_m(A^{-1})_{mn}I_m^{(1)}I_n^{(1)}\ , \tag{A23b}$$

where

$$I_1^{(1)}=\frac{1}{2\pi^2}\int_0^\pi\int_0^\pi dx\,dy\,b_1(x,y)(1-\cos 2y)/D(x,y)\ , \tag{A24a}$$

$$I_2^{(1)}=I_3^{(1)}=\frac{1}{2\pi^2}\int_0^\pi\int_0^\pi dx\,dy\,b_1(x,y)\times(1-\cos x\cos y)/D(x,y)\ , \tag{A24b}$$

$$I_4^{(1)}=I_6^{(1)}=\frac{1}{2\pi^2}\int_0^\pi\int_0^\pi dx\,dy\,b_1(x,y)\times(1-\cos x\cos 3y)/D(x,y)\ , \tag{A24c}$$

$$I_5^{(1)}=\frac{1}{2\pi^2}\int_0^\pi\int_0^\pi dx\,dy\,b_1(x,y)(1-\cos 2x)/D(x,y)\ , \tag{A24d}$$

$$I_7^{(1)}=\frac{1}{2\pi^2}\int_0^\pi\int_0^\pi dx\,dy\,b_1(x,y)(1-\cos 4y)/D(x,y)\ , \tag{A24e}$$

$$I_8^{(1)}=I_9^{(1)}=\frac{1}{2\pi^2}\int_0^\pi\int_0^\pi dx\,dy\,b_1(x,y)\times(1-\cos 2x\cos 2y)/D(x,y)\ . \tag{A24f}$$

For $j'\neq 0$ one can obtain $I_{10}^{(1)}$ by the sum rule

$$I_1^{(1)}+2I_2^{(1)}+j_2(2I_4^{(1)}+I_5^{(1)})+j_3(I_7^{(1)}+2I_8^{(1)})+j'I_{10}^{(1)}=0\ . \tag{A25}$$

APPENDIX B: ZERO-POINT CORRECTIONS TO THE *AF-F-H* MULTICRITICAL POINT

The first-order result in $1/S$ reads[22]

$$E(\mathbf{Q})=E_{\rm cl}(\mathbf{Q})[1+(1/S)]+\Delta\ , \tag{B1}$$

where $E_{\rm cl}(\mathbf{Q})$ is the classical ground-state energy given by Eq. (9) and

$$\Delta=\tfrac{1}{2}\sum_{\mathbf{k}}E_{\mathbf{k}}\ , \tag{B2}$$

where $E_{\mathbf{k}}$ is the spin-wave excitation energy,

$$E_{\mathbf{k}}=\sqrt{S_{\mathbf{k}}D_{\mathbf{k}}}\ , \tag{B3}$$

with

$$S_{\mathbf{k}}=\sum_\alpha 2J_\alpha S\sum_{\delta_\alpha}(\cos\mathbf{Q}\cdot\delta_\alpha-\cos\mathbf{k}\cdot\delta_\alpha)+2J'S\sum_{\delta'}(1-\cos\mathbf{k}\cdot\delta')\ , \tag{B4a}$$

$$D_{\mathbf{k}}=\sum_\alpha 2J_\alpha S\sum_{\delta_\alpha}\cos\mathbf{Q}\cdot\delta_\alpha(1-\cos\mathbf{k}\cdot\delta_\alpha),+2J'S\sum_{\delta'}(1-\cos\mathbf{k}\cdot\delta')\ . \tag{B4b}$$

We notice that Δ in Eq. (B2) is of order $1/S$ with respect to the classical ground-state energy of Eq. (9). We also notice that quantum effects vanish in the ferromagnetic region F of Fig. 1, where $\mathbf{Q}=0$, so

$$E_F=E_{\rm cl}(0)\ . \tag{B5}$$

On the contrary, quantum effects lower the classical ground-state energy of the antiferromagnetic (*AF*) and 120° phases. This fact causes a shift of the classical transition lines *AF-F* and 120°-*F* in both cases reducing the region of stability of the *F* phase.

The ground-state energies of the *AF* and 120° phases are obtained from Eq. (B1) by putting

$$\mathbf{Q}_{AF}=(2\pi/(\sqrt{3}a),0) \tag{B6a}$$

and

$$\mathbf{Q}_{120}=(0,4\pi/(3a))\ . \tag{B6b}$$

The reduced energies [$e=E(\mathbf{Q})/6J_1NS^2$] are

$$e_F=-1-j_2-j_3-\tfrac{1}{3}j'\ , \tag{B7a}$$

$$e_{AF}=\tfrac{1}{3}(1+j_2-3j_3-j')\left[1+\frac{1}{S}\right]+\frac{1}{3S}\frac{1}{\pi^3}\int_0^\pi\int_0^\pi\int_0^\pi dx\,dy\,dz(s_{AF}d_{AF})^{1/2}\ , \tag{B7b}$$

$$e_{120}=(\tfrac{1}{2}-j_2+\tfrac{1}{2}j_3-\tfrac{1}{3}j')\left[1+\frac{1}{S}\right]+\frac{1}{3S}\frac{1}{\pi^3}\int_0^\pi\int_0^\pi\int_0^\pi dx\,dy\,dz(s_{120}d_{120})^{1/2}\ , \tag{B7c}$$

where

$$s_{AF}=-(1+\cos 2y+2\cos x\cos y)-j_2(1+\cos 2x+2\cos x\cos 3y)j_3(3-\cos 4y-2\cos 2x\cos 2y)+j'(1-\cos z), \tag{B8a}$$

$$d_{AF}=-(1+\cos 2y-2\cos x\cos y)-j_2(1+\cos 2x-2\cos x\cos 3y)+j_3(3-\cos 4y-2\cos 2x\cos 2y)+j'(1-\cos z)\ , \tag{B8b}$$

$$s_{120}=-\tfrac{3}{2}-(\cos 2y+2\cos x\cos y)+j_2(3-\cos 2x-2\cos x\cos 3y)-j_3(\tfrac{3}{2}+\cos 4y+2\cos 2x\cos 2y)+j'(1-\cos z)\ , \tag{B8c}$$

$$d_{120}=-\tfrac{1}{2}(3-\cos 2y-2\cos x\cos y)+j_2(3-\cos 2x-2\cos x\cos 3y)-\tfrac{1}{2}j_3(3-\cos 4y-2\cos 2x\cos 2y)+j'(1-\cos z)\ . \tag{B8d}$$

The zero-point motion is well defined only if the argument of the square roots appearing in Eqs. (B8) are nonnegative. This occurs only inside the regions of stability of the corresponding classical phases AF or 120° in Fig. 1.

However, we expect that the shift of the "classical" transition line F-AF in Eq. (2a) and F-120° in Eq. (2c) is of order $1/S$, so that we may correctly give the "quantum" transition lines to order $1/S$ by evaluating the $1/S$ contribution along the "classical" transition lines. The new transition lines are then obtained by comparing Eqs. (B7a) and (B7b) for the F-AF transition and Eqs. (B7a) and (B7c) for the F-120° transition. Thus the F-AF "quantum" transition line is given by

$$j_2=-1+\frac{3j_3}{4S}+\frac{j'}{4S}-\frac{1}{4S\pi^3}\int_0^\pi\int_0^\pi\int_0^\pi dx\,dy\,dz\,(s_{AF}d_{AF})^{1/2}\Big|_{j_2=-1} \tag{B9}$$

for $j_3\geq\frac{1}{2}$. This result is shown in Fig. 7(a) for $S=1$ and in Fig. 7(b) for $S=\frac{5}{2}$ for selected values of the interplane coupling J'. As one can see, the quantum effects are reduced by increasing either the spin S or the interplane coupling J'. The extrapolated triple points A'', for $j'=0,0.1$, and 1 are also shown in Fig. 7, where they can be compared to the first order result in $1/S$ from the t-matrix calculation for the point A' where E_4 vanishes. For $S=\frac{5}{2}$ the existence of a first-order phase transition between the H_1 and F phase seems well established, because all the A' fall well outside the intervals A-A''. The same could be expected for $S=1$ and $J'\neq 0$. Instead, in the extreme quantum limit, $S=\frac{1}{2}$ and $J'\to 0$, the AF phase seems to prevent the first-order phase transition between the H_1 and F phases. The two possible scenarios for the structure of the phase diagram near the F-H-AF multicritical point are shown in Fig. 6.

Now we consider analogously the triple point C. The "quantum" F-120° transition line is given by

$$j_3=-1+\frac{2j_2}{3S}+\frac{2j'}{9S}-\frac{2}{9S\pi^3}\int_0^\pi\int_0^\pi\int_0^\pi dx\,dy\,dz\,(s_{120}d_{120})^{1/2}\Big|_{j_3=-1} \tag{B10}$$

for $j_2\geq 1$. We used this equation to determine the F-120° phase boundary for $j_2>1$. This phase boundary was then extrapolated to find the point A'' where it intersects the classical F-H phase boundary. In all cases we found to order $1/S$ that the point A' on the F-H phase boundary where quantum effects cause e_4 to pass through zero was inside the interval A-A''. Accordingly, the F-H transition remains continuous even near the F-H-120° multicritical point.

*Permanent address: Department of Physics, University of Pennsylvania, Philadelphia, PA 19104.

[1]B. Coqblin, *The Electronic Structure of Rare Earth Metals and Alloys: The Magnetic Rare Earths* (Academic, London, 1977).
[2]E. Rastelli, L. Reatto, and A. Tassi, Physica **97B**, 1 (1979).
[3]A. Adam, D. Billerey, C. Terrier, R. Mainard, L. P. Regnault, J. Rossat-Mignod, and P. Meriel, Solid State Commun. **35**, 1 (1980).
[4]P. Day and K. R. A. Ziebeck, J. Phys. C **13**, L523 (1980).
[5]S. K. Kuindersma, J. P. Sanchez, and C. Haas, Physica **111B**, 231 (1981).
[6]E. Rastelli, L. Reatto, and A. Tassi, J. Phys. C **16**, L331 (1983).
[7]E. Rastelli, L. Reatto, and A. Tassi, J. Phys. C **19**, 6623 (1986).
[8]A. B. Harris and E. Rastelli, J. Phys. C **20**, L741 (1987).
[9]For a square lattice the first terms which depend on θ_Q would appear at order Q^4, but the effect of such anisotropy would similarly discriminate between having the helix wave vector along a FNN direction or along a SNN direction. See also A. B. Harris, A. Pimpinelli, E. Rastelli, and A. Tassi, J. Phys. C **24**, 3821 (1989).
[10]A. B. Harris and E. Rastelli, J. Appl. Phys. **63**, 3083 (1988).
[11]F. J. Dyson, Phys. Rev. **102**, 1217 (1956); **102**, 1230 (1956).
[12]S. V. Maleev, Zh. Eksp. Teor. Fiz. **33**, 1010 (1957) [Sov. Phys.—JETP **6**, 776 (1958)].
[13]J. Goldstone, Proc. R. Soc. London, Ser. A **239**, 267 (1957).
[14]M. Wortis, Phys. Rev. **132**, 85 (1963).
[15]R. Silberglitt and A. B. Harris, Phys. Rev. **174**, 640 (1968).
[16]G. F. Koster, Solid State Phys. **5**, 174 (1957).
[17]P. Day, M. W. Moore, T. E. Wood, D. McK. Paul, K. R. A. Ziebeck, L. P. Regnault, and J.Rossat-Mignod, Solid State Commun. **51**, 627 (1984).
[18]L. P. Regnault, J. Rossat-Mignod, A. Adam, D. Billery, and C.Terrier, J. Phys. (Paris) **43**, 1283 (1982).
[19]A. Adam, D. Billery, C. Terrier, H. Bartholin, L. P. Regnault, and J.Rossat-Mignod, Phys. Lett. **84A**, 24 (1981).
[20]P. Day and C. Vettier, J. Phys. C **14**, L195 (1981).
[21]M. W. Moore and P. Day, J. Solid State Chem. **59**, 23 (1985).
[22]E. Rastelli, L. Reatto, and A. Tassi, J. Phys. C **18**, 353 (1986).